Dissolution of bioactive glass S53P4 in a three-reactor cascade in continuous flow conditions

Siekkinen, Minna; Karlström, Oskar; Hupa, Leena

Published in:
Open Ceramics

DOI:
10.1016/j.oceram.2022.100327

Published: 01/03/2023

Document Version
Final published version

Document License
CC BY-NC-ND

Open Ceramics 13 (2023) 100327

Contents lists available at ScienceDirect

Open Ceramics

journal homepage: www.sciencedirect.com/journal/open-ceramics

Dissolution of bioactive glass S53P4 in a three-reactor cascade in continuous flow conditions

Minna Siekkinen, Oskar Karlström, Leena Hupa *

Johan Gadolin Process Chemistry Centre, Åbo Akademi University, Henrikinkatu 2, 20500, Turku, Finland

ARTICLE INFO

Handling Editor: P Colombo

Keywords:
Bioactive glass
In vitro dissolution
Ion-release
Reaction layer

ABSTRACT

This study expands the knowledge of bioactive glass S53P4 dissolution by implementing a cascade reactor to a continuous dissolution setup. Three reactors were coupled in a series to study the effects of released ions on S53P4 reactions in each reactor. The pH and ion concentrations were measured in Tris-buffer and simulated body fluid flowing through the cascade reactor for five days. The reaction layer formed on the particles in each reactor were also analysed. In Tris, the dissolved Si decreased from 100% to 40% and 26% in the consecutive reactors after five days. In SBF, Si decreased from 64% to 11% and 8%. Thus, the ions released and decrease of available hydrogen ions for ion exchange influenced the dissolution behaviour of S53P4. The results partly explain the differences in the reaction degree between individual bioactive glass particles used as a bone graft in the same defect site.

1. Introduction

Biocompatible materials for repairing or replacing tissue include inert materials, such as metals, and active, such as bioactive, and regenerative materials [1]. A particular category of bioactive implant materials is bioactive glass, used to repair injured or diseased bones since 1985 [2]. Professor Hench and colleagues discovered and developed the first bioactive glass 45S5 in 1969 [2]. Since then, several glass compositions have been proven to gradually dissolve while forming a characteristic hydroxyapatite surface layer in aqueous solutions. This surface layer binds the material with hard and soft tissues [3]. The dissolution of bioactive glasses has been investigated *in vitro* and *in vivo* to verify the bioactivity of different compositions [4–7]. 45S5, also known as Bioglass®, consists of (in wt-%) 45 SiO_2, 24.5 CaO, 24.5 Na_2O, and 6 P_2O_5 [8]. Another clinically used bioactive glass, S53P4, was developed in the 1990s [9]. S53P4 has been reported to show antibacterial properties and have a similar dissolution behaviour as 45S5 [7,10]. The oxide composition of S53P4 is (in wt-%) 53 SiO_2, 20 CaO, 23 Na_2O, and 4 P_2O_5.

In vitro comparison of bioactive glass 45S5 and S53P4 plates showed that S53P4 immersed in static buffered solutions increased the solution pH to a smaller extent than 45S5 [11]. On the other hand, the released Si concentration from the plates after one week was of a similar level for both glasses. S53P4 powder has antibacterial properties against 17 anaerobic and 29 aerobic bacteria [12,13]. The antibacterial properties of S53P4 have been clinically verified, e.g., in treating chronic osteomyelitis of long bones [14]. Further, using S53P4 provided antibacterial properties without the need for additional antibiotic therapies [15]. S53P4 has also been reported as well-tolerated in patients and supports faster healing of chronic osteomyelitis than conventional bone grafts when removing benign bone tumours [16,17]. Both the antibacterial effects and the bone regeneration depend on the ion dissolution rate from the glass. Long-term clinical results also reported residual glass within the well-regenerated bone [17]. The composition of these S53P4 remnants, however, is not known.

The reactions occurring at the bioactive glass surface upon exposure to physiological solutions in the human body or simulated body fluid (SBF) *in vitro* are usually described with the five following steps [18]: (i) exchange of alkali and alkaline ions from the glass with hydrogen ions from the solution and creating silanol bonds on the glass surface, (ii) local increase of solution pH leading to breaking of the glass structure (*Si*–O–Si bonds) and leaching of soluble silicon species to the solution, (iii) formation of a Si-rich layer on the surface as Si–OH groups condensate, (iv) migration of Ca^{2+} and PO_4^{3-} groups from bulk glass and solution to form an amorphous film of CaO–P_2O_5 on the surface, and (v) incorporation of hydroxyls and carbonates from the solution into the film followed by crystallization of the CaO–P_2O_5-film to a hydroxyapatite layer similar to bone apatite. After the hydroxyapatite layer has

* Corresponding author.
E-mail address: leena.hupa@abo.fi (L. Hupa).

https://doi.org/10.1016/j.oceram.2022.100327
Received 4 September 2022; Received in revised form 13 December 2022; Accepted 22 December 2022
Available online 31 December 2022

formed, a series of biological mechanisms result in the bonding to the bone.

In vitro experiments are often performed by immersing either small blocks or particles of the bioactive glass in a static, buffered solution [4,19,20]. As such static tests are conducted in a well-controlled environment, they allow changing parameters to investigate the effect of glass composition, solution, or time on the dissolution behaviour. However, it has been suggested that static studies do not reflect the dynamic environment of the body [21,22] and, as a result, dynamic *in vitro* experiments have been introduced [23]. Since bioactive glasses are highly soluble materials, tests with a circulating solution have been evaluated to avoid solution supersaturation [24]. Some studies replaced the immersion solution SBF with fresh SBF after 6, 24, and 48 h [25] or every day for 28 days [26]. Also circulating the SBF with a flow of 1 ml/min through the sample has been studied [27]. These studies concluded that experiments in replenished or circulating solutions mimic the dynamic body environment better than experiments in static solutions. Furthermore, thinner but more uniform layers formed on particles in tests where the solution was circulated above the particle bed [28,29]. Continuous flow-through reactor with the possibility to adjust the fluid flow rate was developed to study the initial ion release from bioactive glasses into a fresh solution fed through the glass particles [10,30]. In these studies, the glass surface area, particle bed dimensions, flow rate, temperature, and composition of the solution affected the initial ion release from the bioactive glass 1–98 (in wt-% 53 SiO_2, 22 CaO, 6 Na_2O, 2 P_2O_5, 11 K_2O, 5 MgO, and 1 B_2O_3).

The role of surface area on bioactive glass dissolution has been studied using different particle size fractions [31,32]. Smaller particles, i.e., a larger specific surface area, release ions quicker than larger particles, i.e., smaller specific surface area. As the released ions change the local ion concentrations of the surrounding solution, the ions are likely to affect the overall dissolution behaviour of the glass. So far, research focusing on the effect of local ion concentrations on glass dissolution is scarce. Although the solution pH inside a particle bed undergoing dissolution can be measured [28,29], analysing the reaction layers after the experiment is challenging as the particles' location in the bed during the experiment is difficult to trace.

In our recent study, a cascade reactor was used to separate 45S5 particles section-wise into three batches, and the solution was fed through the reactors connected in series [33]. Faster reactions and increased dissolution of particles were identified for particles in the first reactor compared to the second and third reactors. Also, the dissolution of silicon decreased from 92% in the first reactor to 26% and 24% in the second and third reactors after seven days of continuous Tris flow. For dissolution in SBF, the Si release was 35%, 20%, and 19% of the Si in the samples in the three consecutive reactors. Although the experiments with 45S5 in the cascade reactor system with a continuous fluid flow introduced a novel experimental procedure to consider for researching new implantable materials, the understanding of the impact of the local ion concentration on the overall dissolution is still poorly understood.

The present study investigates the impact of dissolved reaction products from the bulk glass, i.e., how the ion concentrations and pH changes in the surrounding solution influence the dissolution behaviour of S53P4 *in vitro*. The experiments were conducted in the cascade reactor system with a continuous flow of Tris and SBF. The ultimate goal was to shed light on the long-term dissolution behaviour of bioactive glasses used as bone grafts.

2. Materials and methods

2.1. Glass particles

S53P4 particles were provided by Bonalive Biomaterials Ltd (Turku, Finland). The wide size range of particles was sieved to a 300–500 μm size fraction. The particles were cleaned with acetone in an ultrasound bath until the acetone stayed transparent after the cleaning, to remove powder adhered to the particle surfaces. Fig. 1 presents (a) the particle size distribution (Malvern Panalytical Mastersized 3000) and (b) an SEM image of the unreacted glass particles. The average diameter was 500 μm, and 57% of the particles had a diameter between 272 and 515 μm. Due to the irregular shapes of the crushed glass particles, some elongated particles could pass through the 500 μm sieve, influencing the size distribution. It should be noted that the SEM image in Fig. 1 represents particle cross-sections taken in a random location of a particle bed.

2.2. Buffer solution preparation

The *in vitro* studies were conducted in simulated body fluid (SBF) [34] and tris(hydroxymethyl)aminomethane (Tris) and were prepared in-house. SBF is considered to mimic the reactions occurring *in vivo* more effectively than sole Tris, due to its similar content of inorganic ions as human blood plasma. However, as SBF already contains high concentrations of some inorganic ions, supersaturation during the ion release from the glass may be an issue [35]. The Tris-buffered SBF was prepared according to ISO 23317:2014 [36] by adding each chemical (Table 1) into 850 ml of purified water in a beaker with a magnet continuously stirring throughout the dissolution. The Tris-buffer for SBF was separately dissolved in a small amount of purified water before slowly being added to the solution with the inorganic ions. Before adjusting the pH, the solutions were kept at 37 °C in a water bath for 4 h (SBF) and 2 h (Tris). The pH was adjusted by adding 1 M HCl into the buffered solutions until the pH was 7.4 at 37 °C. The solutions were transferred to a volumetric flask into which purified water was added to obtain the correct volume. The solution volumes were temperature-adjusted at room temperature.

2.3. Experimental setup

The experiments were conducted in a cascade setup consisting of three reactors connected in series with a continuous flow of the buffered solutions through the reactors. A detailed description of the setup can be found elsewhere [30,33,37]. The three reactors were assumed to represent different locations of dissolving particles in a bed. The glass particles in the first reactor were assumed to represent those with the first contact with the solution. Correspondingly, the particles in the second reactor would correlate to the bulk phase particles. Finally, the third reactor particles were assumed to have experienced a similar environment as the innermost particles in a single bed. 205 ± 5 mg S53P4 glass particles were added to each reactor.

A peristaltic pump fed the buffer solution through the cascade reactor system with a 0.2 ml/min flow rate. Thin thermoplastic Tygon® tubes connected the solution to the inflows and outflows from the reactors. The solution and reactors were kept in a 37 °C water bath to mimic the temperature inside the human body. After one, two, and all three reactors, the outflow solution was collected into test vials at various time points for 20 min to provide a total solution of 4 ml for further analyses. The solutions were collected every 20 min for the first hour and then at 2, 4, 6, 8, 16, and 24 h. After 24 h, the solution was collected every 24 h for 5 days. Additionally, 1 ml of the bulk solution outflow between each measurement point was collected for further ion analysis. Three parallel runs were conducted for experiments up to 5 days. Several samples of the buffer solution were used to obtain its average pH and initial inorganic ion concentrations. The cross-sections of partially reacted glass particles were analysed at 4, 24, and 72 h.

2.4. Temperature and pH

The temperature and pH (Mettler Toledo SevenEasy S20) were measured directly after collecting the solution from the outflow. As the solution temperature rapidly decreased to room temperature, the values were calculated to give the pH at 37 °C using equation (1) [38]. The equation was verified by measuring the pH of the reference solution at

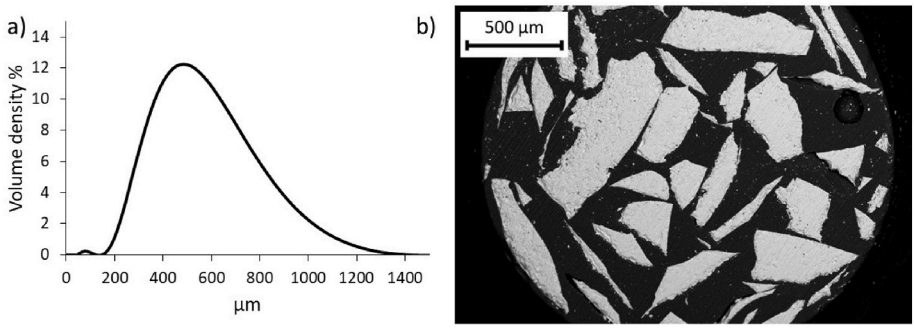

Fig. 1. Particle size distribution (a) and SEM image of unreacted S53P4 particles (b).

Table 1
Concentrations (g/l) of chemicals in SBF and Tris buffer solutions.

	NaCl	$NaHCO_3$	KCl	$K_2HPO_4{\cdot}3H_2O$	$MgCl_2{\cdot}6H_2O$	1 M HCl (aq)	$CaCl_2{\cdot}2H_2O$	Na_2SO_4	Tris
SBF	7.996	0.35	0.224	0.228	0.305	35 ml	0.368	0.071	6.057
Tris	–	–	–	–	–	–	–	–	6.057
Manufacturer	*VWR Chemicals*	*J.T. Baker*	*Sigma Aldrich*	*Sigma Aldrich*	*Sigma Aldrich*	*Sigma Aldrich*	*VWR Chemicals*	*Sigma Aldrich*	*Sigma Aldrich*

different temperatures in a water bath. Calibration of the pH meter was done with standardized buffer solutions with pH 4.01, 7.00, and 9.21.

$$pH_{37} = pH_{measured} - 0.02664 * (37 - T_{measured}) \quad \text{Eq 1}$$

2.5. Ion analysis

The concentrations of Si, Ca, Na, and P species in the collected solutions were analysed with inductively coupled plasma optical emission spectroscopy (ICP-OES, Optima 5300 DV; PerkinElmer, Waltham, MA). Three parallel samples were performed at each time point. The limits of quantification of the analysed ions were 0.004 mg/l for Si, 0.03 mg/l for Ca, 0.2 mg/l for Na, and 0.03 mg/l for P. The wavelengths for the conducted analyses were 251.622 nm for Si, 317.933 for Ca, 589.592 nm for Na, and 213.617 for P. The collected solutions were diluted in the volume ratio of 1:10 before the ICP-OES analysis. The ICP-OES was calibrated with ultrapure water and a commercial multi-element standard (Spectrascan) with 1, 5 and 20 ppm Si, Ca, Na, and P. The calibration was verified by measuring the ion concentrations of the multi-element standard after every 60 samples. The background level was recorded before each sample run. All reported ion concentrations are background corrected.

2.6. Reaction layers on particle surfaces

The reaction layers on the particle surfaces were analysed with a scanning electron microscope with energy dispersive x-ray analysis (SEM-EDX, Leo Gemini; Carl Zeiss, Oberkochen, Germany). For this, the partly dissolved particles were removed from the reactors, washed with

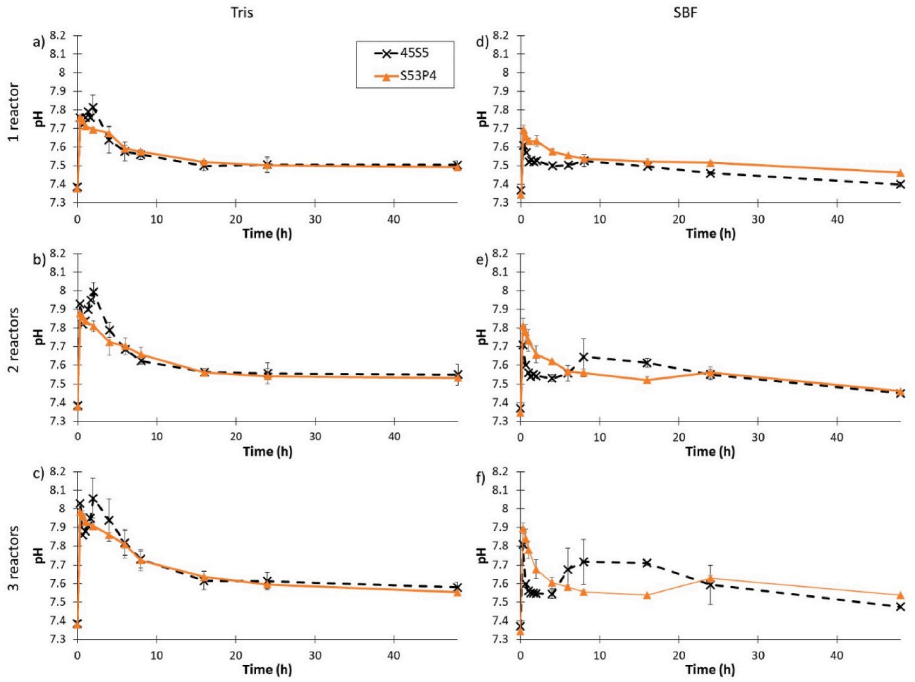

Fig. 2. The pH changes as functions of time for experiments conducted in Tris (left) and SBF (right) for the consecutive reactors with S53P4 and 45S5 [33].

ethanol to stop the reactions, dried at 40 °C in an oven overnight, and then embedded into epoxy resin. The cross-sectional areas of the particles were obtained by grinding and polishing the epoxy-embedded particles.

3. Results

3.1. Influence of glass dissolution on pH

Fig. 2 shows the pH changes during the first 48 h of dissolution of S53P4 particles in Tris (left) and SBF (right) after each reactor in the cascade reactor system, with an increasing number of reactors arranged vertically. The figure also displays the corresponding data for 45S5 [33]. For all reactors, pH first increased to 7.6–8, followed by a decrease in both solutions. In SBF, the pH first decreased more rapidly than in Tris. Between 2 and 8 h, the pH decreased similarly in Tris and SBF. Interestingly, a second increase and decrease of pH in SBF can be observed after multiple reactors at around 24 h for S53P4. After 24 h, the pH of Tris stabilized in all reactors and the first reactor in SBF. The stabilization of the pH took longer for the second and third reactors.

In Tris and SBF, the initial pH increases were consistently highest after all three reactors and lowest after the first reactor. Also, the pH increased with the number of reactors at all times. However, the total pH increases between the solution inflows and outflows were lowest for the second and third reactors, and highest for the first reactor. In Tris, the highest pH increase compared to the inflow pH was at 20 min (0.33 h) with the total increases as follows: 0.38 pH units (1st reactor); 0.12 (2nd reactor); 0.10 (3rd reactor). The corresponding pH differences in SBF were: 0.34; 0.12; 0.09.

3.2. Ion release

Fig. 3 shows the ion concentrations in the solutions after each reactor as functions of time. The highest Ca, Na, and P concentrations in Tris were measured at 20 min (the first measuring point). On the other hand, the highest Si concentration was measured at shorter dissolution times for increasing number of reactors according to 2 h, 40 min, and 20 min. In SBF, the highest Si concentration was measured at 1 h after one and two reactors and at 20 min after all three reactors. The highest Ca concentration in SBF was measured at 20 min for all reactors. The high initial Na concentration in SBF prevented accurate simultaneous analyses with the other ions. Thus, the reported Na concentrations released from the glass into SBF are only indicative. The highest Na concentrations were measured at 120 h in the first and second reactors. For three reactors, the highest Na concentration was measured already at 20 min. Correspondingly, the highest P concentrations in SBF were measured at 20–60 min after the two first reactors and at 2 h after all three reactors. Noticeably, the highest P concentrations in SBF were measured after one reactor, followed by all three reactors. The relatively low initial P content of the unreacted S53P4 was assumed to provide only minor changes

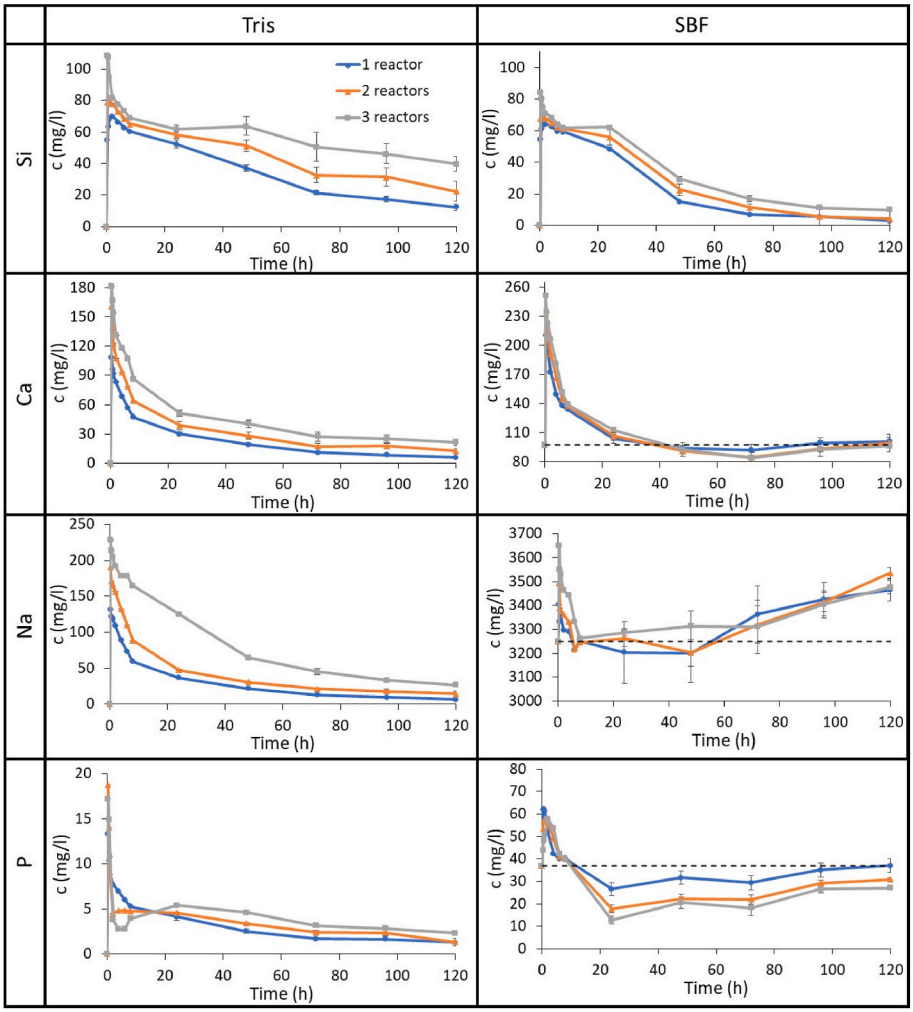

Fig. 3. Average concentrations of Si, Ca, Na and P species released into Tris and SBF in the three consecutive reactors as functions of dissolution time. The standard deviations are shown for the analyses from 24 h onward. The dashed lines give the initial concentrations in SBF.

in the ion concentration of the solution, thus influencing the accuracy of the measurements.

The changes in Si concentration in Tris and SBF after each reactor are presented in Fig. 4. The figure also includes results of 45S5 under similar conditions [33]. The values for S53P4 were calculated from the Si concentrations (mg/l) given in Fig. 3. In general, the Si trends were similar for both Tris and SBF. The highest Si concentrations were observed in the first reactor in both solutions and for both glasses. For S53P4, it should be noted that the Si concentration decreased more rapidly in SBF than in Tris. On the other hand, the decrease of Si concentration was more rapid in Tris than SBF for 45S5. However, the Si concentration in Tris for 45S5 was stable at around 25 mg/l after the decrease. A similar stabilization level for S53P4 was also seen in Tris, but the decrease was less rapid than for 45S5. For the second and third reactors, the first 48 h show apparent differences between S53P4 and 45S5. In both Tris and SBF, the biggest change of Si concentration can be seen for the first measuring point for S53P4, while for 45S5, the high and broad peak of the change of Si concentration can be seen between 8 and 48 h in SBF.

3.3. Reaction layers

SEM images of S53P4 after dissolutions in Tris and SBF for 4, 24, and 72 h are shown in Figs. 5 and 6. Already at 4 h in Tris, thin silica-rich (Si-rich) layers (light grey) are visible for particles from the first and second reactors. At 4 h, no surface layer can be seen on the particles in the third reactor in Tris or any of the reactors in SBF. At 24 h, distinct Si-rich layers and indications of calcium phosphate (Ca/P) layers are seen on some particles in all reactors in Tris and SBF. However, the SEM images and line imply that surface layers formed in Tris were indistinct.

The line analyses (EDX) close to the external surface of separate particles is shown in Fig. 5 for S53P4 particles after dissolution in Tris for 4, 24, and 72 h. Particles from the first and second reactors have a silica-rich layer at 4 h, while no layers can be seen on glass particles taken from the third reactor. The line analysis along the particle surface cross-section shows the silica-rich layer as increased Si and decreased Ca, Na, and P contents. The Na content is almost constant in the unreacted particle parts below the surface layer. With increasing dissolution times, the thickness of the Si-rich layer increased. Also, the Ca and P concentrations at the outermost surface increased. At 72 h, Ca and P increased within the Si-rich layer. This mixed Si-rich + Ca/P layer was more pronounced in the second and third reactors than in the first. These analyses suggest that no pure Ca/P outer surface layer had formed on the particles in Tris in any of the investigated cases.

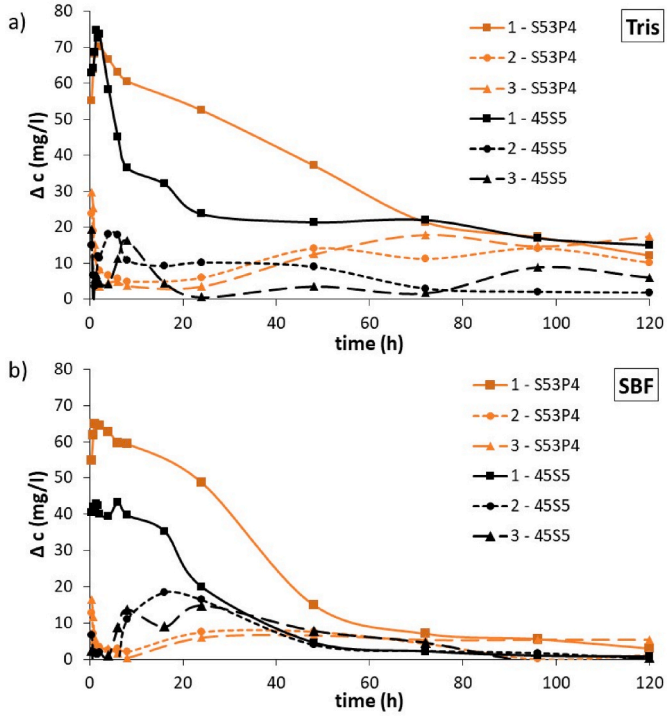

Fig. 4. Si concentration change in Tris (above) and SBF (below) after each reactor for S53P4 and 45S5 [33].

The EDX-line analyses of S53P4 particles after dissolution in SBF for 4, 24, and 72 h is shown in Fig. 6. No layers can be seen in particles from any reactor at 4 h, implying that the reaction layers formed later. The line analyses also show an almost constant concentration of the elements throughout the particle cross-section in all reactors. However, after 24 h in SBF, distinct Si-rich layers can be seen on particles from all reactors. Additionally, a mixed layer consisting of Ca/P and Si, followed by a Ca/P outer surface layer can be noticed in the first and second reactor particles. The line analyses also confirm the Ca/P layer in this case; the Si content decreases towards zero, while only Ca and P are present on the outer surface. On the other hand, only a mixed layer of Ca/P and Si was analysed on the third reactor particles.

Between 24 and 72 h, the reaction layer thickness increased in SBF. The first reactor particles display a distinct Si-rich layer, indications of a mixed layer, and an extensive outer, almost pure Ca/P-layer. The analysed particle in the second reactor showed similar but notably thinner layers. Finally, the analysed particle in the third reactor showed an uneven Si-rich layer, a mixed layer, and a thin pure Ca/P-layer.

The EDX line analyses along the particle surfaces in Figs. 5 and 6, show increases in the Ca and P contents after 24 and 72 h in Tris and SBF. In Tris, Ca and P increases are accompanied by Si. In contrast, the outer layer consisted of almost pure Ca/P, with Si and Na close to zero after SBF dissolution. At 24 h and onward, only the third reactor particles showed a mixed layer of Si, Ca, and P in SBF. These results suggest that the phosphate content released in Tris was not high enough to form a pure Ca/P layer on the S53P4 particles. Instead, a mixed layer formed in Tris. In contrast, the particles had visibly fused by the outermost Ca/P layer after 120 h in SBF.

4. Discussion

Highly reactive materials, such as bioactive glasses, release ions when in contact with physiological solutions. However, the role of the released ions on the dissolution of bioactive glasses has been poorly studied. Only a few studies discuss the impact of the dissolution products. The main emphasis has been on the cellular responses to the dissolution products from the dissolved bioactive glass [39–41]. For example, dissolution products from bioactive glass 45S5 have been shown to shorten the human osteoblast growth cycle [40].

In an earlier study, we showed that a cascade reactor could be utilized in the continuous dissolution flow-through to investigate the release of ions between each section of a larger implanted particle bed [33]. The ability of bioactive glasses to exchange ions with the surrounding solution is one of the most distinctive properties of the material and is correlated to the pH increase. In this study, an increasing number of reactors increased the pH of the solution flowing through the bioactive glass particles (Fig. 2), indicating that fewer hydrogen ions were available for ion exchange with the particles. Consequently, this led to delayed reactions between material and solution in subsequent reactors. The impact of the reaction products on the dissolution of bioactive glasses was especially noticeable in SBF. Interestingly, with added reactors in SBF, a second increase in the pH was seen for S53P4 and 45S5. This indicates that the reaction products delayed the solution-material reactions as the increase of pH is one of the earliest steps of the reaction behaviour. However, the second increase was measured later for S53P4 than 45S5 (at 24 h compared to 8 h). For S53P4, there is a dramatic decrease of P in SBF between 8 and 24 h (Fig. 3). The lowest levels of P concentrations were measured in SBF at

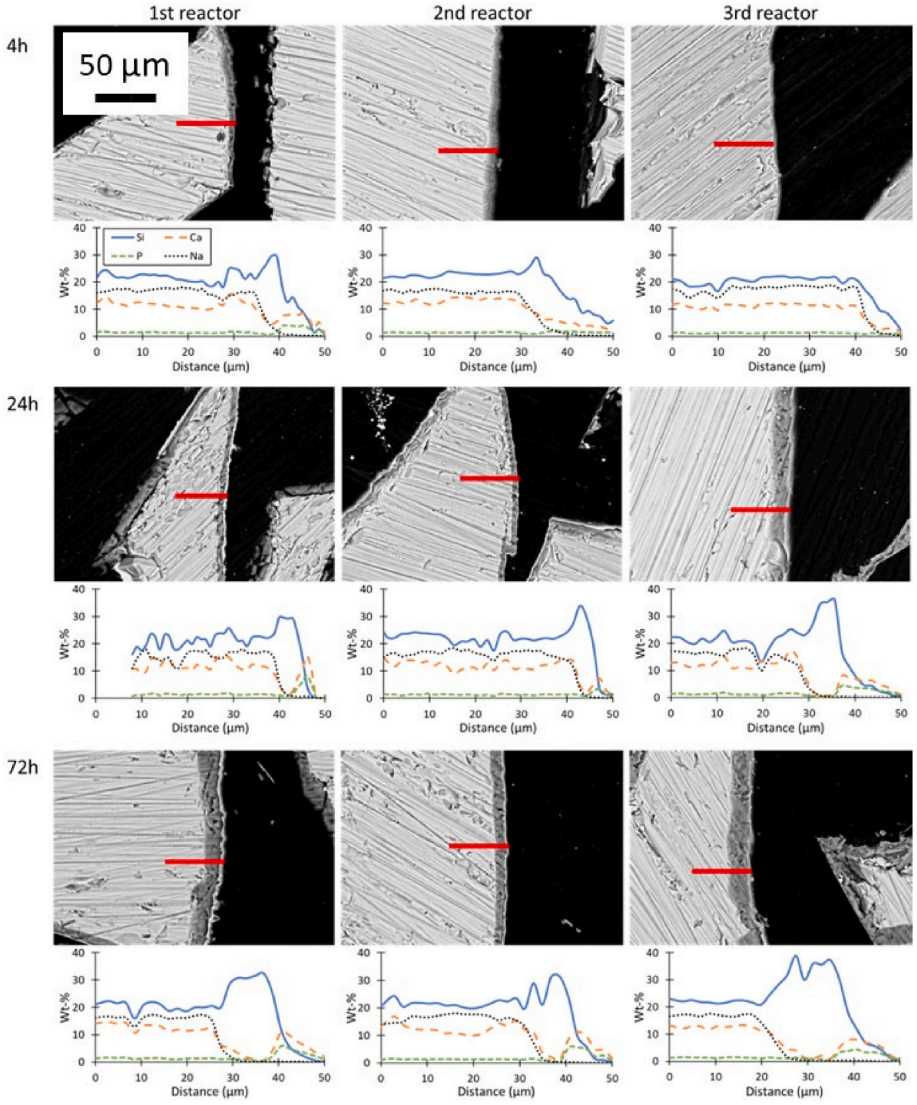

Fig. 5. SEM images and EDX-analyses of S53P4 particle cross-sections after different dissolution times in a continuous flow of Tris.

24 h as 27 mg/l after one reactor, 18 mg/l after two reactors, and 13 mg/l after all three reactors. Only after the first reactor did the P concentration at 120 h increase to the measured P levels in the reference SBF. Whereas for 45S5, a similar P decrease was seen earlier, between 6 and 8 h of continuous dissolution. A decrease in the P species concentration of SBF is usually seen in static experiments when the phosphate in the solution precipitates on the material surfaces [42]. However, precipitation of Ca/P starts at established nucleation sites (Si-rich layer). The decrease of P in the inflow to the second and third reactors indicate that P in the SBF precipitates in the first reactor as soon as a suitable nucleation site is present. As particles in the later reactors lack the Si-rich layer during the first hours, Ca/P cannot precipitate from the solution rich in P. Reaction layers, especially the outer Ca/P layer, are crucial for bonding to the bone *in vivo* [43]. In SBF (Fig. 6), a pure outer Ca/P layer can be seen from the line analyses in the two first reactors at 72 h, whereas the outer Ca/P layer in the third reactor suggests decreasing Si concentrations along the line. In Tris (Fig. 5), similar mixed Si and Ca/P layer could be seen at 72 h in all reactors. Similar reaction patterns were identified for 45S5 in the cascade reactor [33].

Fig. 7 shows the cumulative dissolution of Si from S53P4 and earlier studied 45S5 [33]. The cumulative dissolution is calculated from data in Fig. 3, the volume of the solution fed through the system, and the amount of Si in the unreacted bioactive glass sample placed in the reactors. Overall Si-release from S53P4 and 45S5 into the two solutions correlated with the total SiO_2 content in the glasses. A high Si release from the first reactor particles decreased the concentration gradients around the particles in the consecutive reactors, thus leading to lower cumulative Si dissolution. Although S53P4 has a higher concentration of Si-species available for dissolution, the glass also has higher chemical durability. Accordingly, Si-rich and Ca/P layers formed slower on S53P4 than on 45S5 particles. Thicker Si-rich and Ca/P layers more effectively decreased the Si-release from the 45S5 particles to both solutions [33]. The large differences in the cumulative Si-release from S53P4 between the first and the two consecutive reactors were assumed to depend on a combined effect of chemical durability, higher concentration gradients around the second and third reactor particles, and also, to some degree, the Ca/P layers retarding the Si-species diffusion from the bulk glass. Thus, larger differences were measured between the S53P4 particles in the three reactors than reported for 45S5. However, the trends measured for S53P4 were similar to 45S5, verifying the impact of local ion concentrations on bioactive glass dissolution. The release of all ions from S53P4 increased with an increased number of reactors (Fig. 3). However, when comparing Si concentrations after each reactor, the decrease in the release was not proportional to the sample amount in the reactor (Fig. 4). The Si concentrations in the outflows from the second and third reactors were almost identical when correlated to the Si concentration in

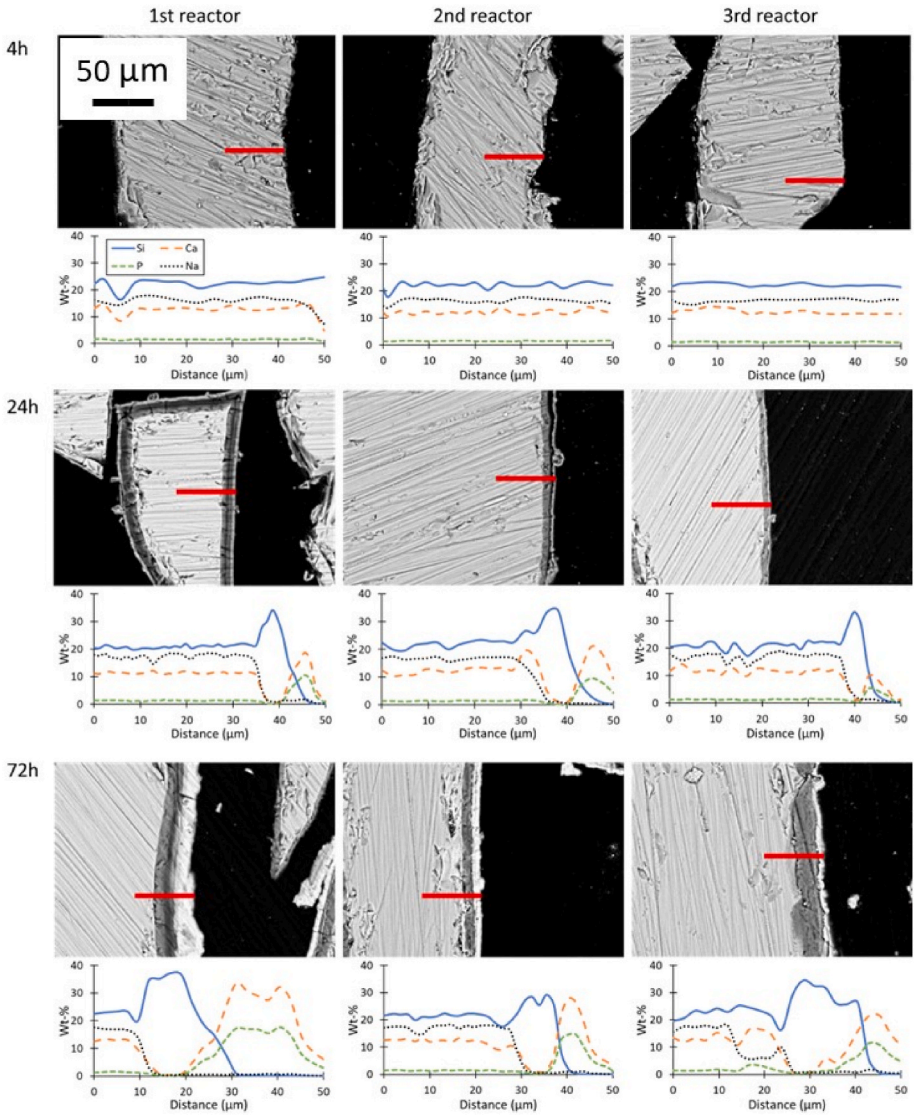

Fig. 6. SEM images and EDX-analyses of S53P4 particle cross-sections after different dissolution times in a continuous flow of SBF.

the inflow. At 72 h, 39.8 mg of the total 50.8 mg Si in the first reactor was dissolved. Corresponding amounts were 11 mg from the second reactor and 7.4 mg from the third reactor. In SBF, the release of Si decreased from 29.1 to 5.2 and 1.9 mg from the three consecutive reactors. The dissolved Si from the first reactor is thus suggested to slow down the further dissolution of Si in the second and third reactors. This effect is likely due to soluble Si species in the solutions being close to saturation levels in the second and third reactors.

S53P4 contains 8 wt-% more SiO_2 than 45S5, indicating that more Si can be released from S53P4 (in this study 50.8 mg Si in S53P4 and 44.9 mg in 45S5 in each reactor). S53P4 has been shown to initially dissolve slower than 45S5 in static conditions [11,44]. However, S53P4 has been reported to show a more consistent dissolution over a two-week immersion test than 45S5. Further, S53P4 dissolved more in Tris than in SBF [11]. In the present work, the Si release was higher from S53P4 than 45S5 in prolonged continuous flow experiments in Tris. Similar trends were measured in SBF for only one reactor. However, more Si was released from 45S5 than S53P4 in multiple reactors (Fig. 7).

The role of pH on bioactive glass dissolution has also been studied. Precipitation of Ca and P species has been demonstrated to occur more rapidly on 45S5 upon immersion at increasing pH in static conditions [45]. The precipitated Ca and P on the glass surface simultaneously decreased the ion release from the bulk glass. Hence, the release of Ca and P is expected to increase at decreased pH, as reported in acidic solutions [46]. Si release also increases with pH due to the ion exchange between the solution and the glass [18,47]. In this work, the solution pH after each reactor was still within the buffering range of the solutions, thus partly explaining that the Si release rate slowed down with dissolution time. However, all Si was dissolved from the S53P4 in the first reactor into Tris at 120 h (Fig. 7). This can be explained by the thin Ca/P layer and the Si species concentration being below the saturation level.

Even though it has been proposed that released ions hinder the dissolution of bioactive glasses, the dissolution products only initially slowed down the dissolution in this work. However, as soon as the bioactive glass particles in the first reactor had developed a Ca/P reaction layer, the dissolution of Si increased in the next reactors. After the Ca/P layer had formed on the first reactor particles, it retarded their further dissolution. Thus, Si concentration gradients around the particles in the following reactors increased, leading to increased Si dissolution.

The results suggest that the released ions strongly affect the dissolution rate of bioactive glasses. Small changes in local ion concentrations had a dramatic effect on the dissolution of S53P4 and 45S5 in SBF. This implies that a larger implanted particle bed may be expected to react non-uniformly *in vivo* under similar flow conditions as reported in this work. However, Fig. 6 shows that an outer pure Ca/P layer had formed

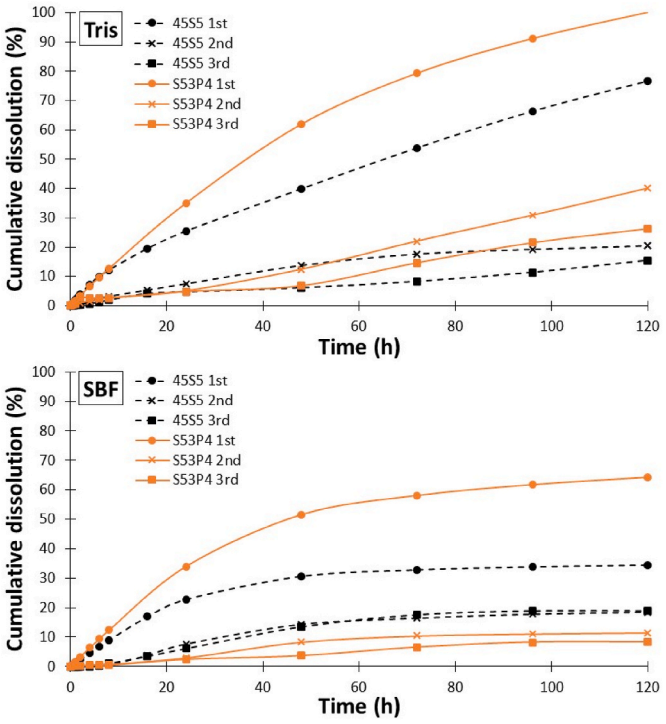

Fig. 7. Cumulative dissolution of silicon (%) from the bioactive glass particles 45S5 and S53P4 in each reactor with experiments conducted with Tris (above) and SBF (below). (For interpretation of the references to colour in this figure legend, the reader is referred to the Web version of this article.)

even in the third reactor particles at 72 h. Thus, these areas representing the conditions inside the particle bed, or the interior part of a porous implant, are gradually covered by Ca/P. This layer can then develop into hydroxyapatite and further convert into bone tissue.

5. Conclusion

This study investigated the effect of released ionic species on the dissolution and reaction layer formation on bioactive glass S53P4 particles in a three-reactor cascade in continuous flow conditions. The released ions from the glass particles in the first reactor influenced the dissolution of the particles in the consecutive reactors. The ion release occurred more rapidly in the first reactor representing the exterior surfaces of an implanted particle bed. In contrast, the increased ion concentrations in solution inflows to the second and third reactors, representing the interior surfaces of the particle bed, led to markedly slower dissolution. Si-rich and Ca/P surface layers developed more rapidly in the first reactor particles than particles in the following two reactors. After a Ca/P layer had formed, the dissolution slowed down. The results imply that the increased local ion concentrations delay reactions in the interior parts of implanted particle beds. Finally, the cascade reactor system provided additional confidence to the established static and dynamic dissolution tests.

Summary of novel conclusions Turku, 17.8.2022

This work enhances the understanding of the *in vitro* reactions of bioactive glass S53P4 particles in different locations of a particle bed in continuous fluid flow. This approach simulates the actual conditions, e.g., grafting bone cavities with bioactive glass particles. When a fresh fluid, such as the co-called simulated body fluid, is fed through the particles, the ions released from the particles with the first contact affect the reactions of the other particles. As the particles were separated into three different reactors in series, the reactions could be studied individually for each reactor. The results showed that the dissolution of bioactive glass in later reactors were affected by the ions released from the first reactor. The results provide new knowledge on the gradual degradation patterns of implanted bioactive glass particles or porous bodies.

Declaration of competing interest

The authors declare that they have no known competing financial interests or personal relationships that could have appeared to influence the work reported in this paper.

Acknowledgements

This work is part of the Business Finland project Smart materials at biomaterial interface (882/31/2019). BonAlive Biomaterials Ltd is acknowledged for material and collaboration. Financial support by Svenska Kulturfonden Project 157767 (Minna Siekkinen) and The Academy of Finland Project 321598 (Oskar Karlström) are acknowledged. Luis Bezerra and Linus Silvander are acknowledged for their technical assistance with ICP-OES and SEM.

References

[1] G.-I. Im, Biomaterials in orthopaedics: the past and future with immune modulation, Biomater. Res. 24 (2020) 7, https://doi.org/10.1186/s40824-020-0185-7.
[2] L. Hench, The story of Bioglass, J. Mater. Sci. Mater. Med. 17 (2006) 967–978, https://doi.org/10.1007/s10856-006-0432-z.
[3] L.L. Hench, G.P. LaTorre, Ö.H. Andersson, The kinetics of bioactive ceramics Part III: surface reactions for bioactive glasses compared with an inactive glass, Bioceramics, Elsevier Ltd (1991) 155–162, https://doi.org/10.1016/B978-0-7506-0269-3.50025-6.
[4] A.L.B. Maçon, T.B. Kim, E.M. Valliant, K. Goetschius, R.K. Brow, D.E. Day, et al., A unified in vitro evaluation for apatite-forming ability of bioactive glasses and their variants, J. Mater. Sci. Mater. Med. 26 (2015) 115, https://doi.org/10.1007/s10856-015-5403-9.
[5] A. Anand, V. Lalzawmliana, V. Kumar, P. Das, K.B. Devi, A.K. Maji, et al., Preparation and in vivo biocompatibility studies of different mesoporous bioactive glasses, J. Mech. Behav. Biomed. Mater. 89 (2019) 89–98, https://doi.org/10.1016/j.jmbbm.2018.09.024.
[6] P.K. Vallittu, J.P. Posti, J.M. Piitulainen, W. Serlo, J.A. Määttä, T.J. Heino, et al., Biomaterial and implant induced ossification: in vitro and in vivo findings, J Tissue Eng Regen Med 14 (2020) 1157–1168, https://doi.org/10.1002/term.3056.
[7] Ö.H. Andersson, I. Kangasniemi, Calcium phosphate formation at the surface of bioactive glass in vitro, J. Biomed. Mater. Res. 25 (1991) 1019–1030, https://doi.org/10.1002/jbm.820250808.
[8] L.L. Hench, Chronology of bioactive glass development and clinical applications, New J. Glass Ceram. 3 (2013) 67–73, https://doi.org/10.4236/njgc.2013.32011.
[9] Ö.H. Andersson, G. Liu, K.H. Karlsson, L. Niemi, J. Miettinen, J. Juhanoja, In vivo behaviour of glasses in the SiO2-Na2O-CaO-P2O5-Al2O3-B2O3 system, J. Mater. Sci. Mater. Med. 1 (1990) 219–227, https://doi.org/10.1007/BF00701080.
[10] S. Fagerlund, L. Hupa, M. Hupa, Dissolution patterns of biocompatible glasses in 2-amino-2-hydroxymethyl-propane-1,3-diol (Tris) buffer, Acta Biomater. 9 (2013) 5400–5410, https://doi.org/10.1016/j.actbio.2012.08.051.
[11] L. Varila, S. Fagerlund, T. Lehtonen, J. Tuominen, L. Hupa, Surface reactions of bioactive glasses in buffered solutions, J. Eur. Ceram. Soc. 32 (2012) 2757–2763, https://doi.org/10.1016/j.jeurceramsoc.2012.01.025.
[12] O. Leppäranta, M. Vaahtio, T. Peltola, D. Zhang, L. Hupa, M. Hupa, et al., Antibacterial effect of bioactive glasses on clinically important anaerobic bacteria in vitro, J. Mater. Sci. Mater. Med. 19 (2007), https://doi.org/10.1007/s10856-007-3018-5.
[13] E. Munukka, O. Leppäranta, M. Korkeamäki, M. Vaahtio, T. Peltola, D. Zhang, et al., Bactericidal effects of bioactive glasses on clinically important aerobic bacteria, J. Mater. Sci. Mater. Med. 19 (2008) 27–32, https://doi.org/10.1007/s10856-007-3143-1.
[14] L. Drago, D. Romanò, E. De Vecchi, C. Vassena, N. Logoluso, R. Mattina, et al., Bioactive glass BAG-S53P4 for the adjunctive treatment of chronic osteomyelitis of the long bones: an in vitro and prospective clinical study, BMC Infect. Dis. 13 (2013) 584, https://doi.org/10.1186/1471-2334-13-584.
[15] M.T. Cunha, M.A. Murça, S. Nigro, G.B. Klautau, M.J.C. Salles, In vitro antibacterial activity of bioactive glass S53P4 on multiresistant pathogens causing osteomyelitis and prosthetic joint infection, BMC Infect. Dis. 18 (2018), https://doi.org/10.1186/s12879-018-3069-x.
[16] N.C. Lindfors, P. Hyvönen, M. Nyyssönen, M. Kirjavainen, J. Kankare, E. Gullichsen, et al., Bioactive glass S53P4 as bone graft substitute in treatment of osteomyelitis, Bone 47 (2010) 212–218, https://doi.org/10.1016/j.bone.2010.05.030.

[17] N.C. Lindfors, I. Koski, J.T. Heikkilä, K. Mattila, A.J. Aho, A prospective randomized 14-year follow-up study of bioactive glass and autogenous bone as bone graft substitutes in benign bone tumors, J. Biomed. Mater. Res. B Appl. Biomater. 94B (2010) 157–164, https://doi.org/10.1002/jbm.b.31636.
[18] J.R. Jones, Review of bioactive glass: from Hench to hybrids, Acta Biomater. 9 (2013) 4457–4486, https://doi.org/10.1016/j.actbio.2012.08.023.
[19] T. Kokubo, H. Kushitani, C. Ohtsuki, S. Sakka, T. Yamamuro, Chemical reaction of bioactive glass and glass-ceramics with simulated body fluid, J. Mater. Sci. Mater. Med. 3 (1992) 79–83, https://doi.org/10.1007/BF00705272.
[20] J. Massera, L. Hupa, M. Hupa, Influence of the partial substitution of CaO with MgO on the thermal properties and in vitro reactivity of the bioactive glass S53P4, J. Non-Cryst. Solids 358 (2012) 2701–2707, https://doi.org/10.1016/j.jnoncrysol.2012.06.032.
[21] A.H. De Aza, P. Velásquez, M.I. Alemany, P. Pena, P.N. De Aza, In situ bone-like apatite formation from a Bioeutectic® ceramic in SBF dynamic flow, J. Am. Ceram. Soc. 90 (2007) 1200–1207, https://doi.org/10.1111/j.1551-2916.2007.01534.x.
[22] Y.R. Duan, Z.R. Zhang, C.Y. Wang, J.Y. Chen, X.D. Zhang, Dynamic study of calcium phosphate formation on porous HA/TCP ceramics, J. Mater. Sci. Mater. Med. 15 (2004) 1205–1211, https://doi.org/10.1007/s10856-004-5673-0.
[23] S. Taipale, P. Ek, M. Hupa, L. Hupa, Continuous measurement of the dissolution rate of ions from glasses, Adv. Mater. Res. 39–40 (2008) 341–346, https://doi.org/10.4028/www.scientific.net/AMR.39-40.341.
[24] D. Rohanová, D. Horkavcová, A. Helebrant, A.R. Boccaccini, Assessment of in vitro testing approaches for bioactive inorganic materials, J. Non-Cryst. Solids 432 (2016) 53–59, https://doi.org/10.1016/j.jnoncrysol.2015.03.016.
[25] G. Theodorou, O.M. Goudouri, E. Kontonasaki, X. Chatzistavrou, L. Papadopoulou, N. Kantiranis, et al., Comparative bioactivity study of 45S5 and 58S bioglasses in organic and inorganic environment, Bioceram. Dev. Appl. 1 (2011) 1–4, https://doi.org/10.4303/bda/D110154.
[26] Y. Zhang, M. Mizuno, M. Yanagisawa, H. Takadama, Bioactive behaviors of porous apatite- and wollastonite-containing glass-ceramic in two kinds of simulated body fluid, J. Mater. Res. 18 (2003) 433–441, https://doi.org/10.1557/JMR.2003.0055.
[27] S. Yue, P.D. Lee, G. Poologasundarampillai, J.R. Jones, Evaluation of 3-D bioactive glass scaffolds dissolution in a perfusion flow system with X-ray microtomography, Acta Biomater. 7 (2011) 2637–2643, https://doi.org/10.1016/j.actbio.2011.02.009.
[28] D. Zhang, M. Hupa, L. Hupa, In situ pH within particle beds of bioactive glasses, Acta Biomater. 4 (2008) 1498–1505, https://doi.org/10.1016/j.actbio.2008.04.007.
[29] D. Zhang, M. Hupa, H.T. Aro, L. Hupa, Influence of fluid circulation on in vitro reactivity of bioactive glass particles, Mater. Chem. Phys. 111 (2008) 497–502, https://doi.org/10.1016/j.matchemphys.2008.04.055.
[30] S. Fagerlund, P. Ek, L. Hupa, M. Hupa, Dissolution kinetics of a bioactive glass by continuous measurement, J. Am. Ceram. Soc. 95 (2012) 3130–3137, https://doi.org/10.1111/j.1551-2916.2012.05374.x.
[31] M.G. Cerruti, D. Greenspan, K. Powers, An analytical model for the dissolution of different particle size samples of Bioglass ® in TRIS-buffered solution, Biomaterials 26 (2005) 4903–4911, https://doi.org/10.1016/j.biomaterials.2005.01.013.
[32] P. Sepulveda, J.R. Jones, L.L. Hench, In vitro dissolution of melt-derived 45S5 and sol-gel derived 58S bioactive glasses, J. Biomed. Mater. Res. 6 (2002) 301–311, https://doi.org/10.1002/jbm.10207.
[33] M. Siekkinen, O. Karlström, L. Hupa, Effect of local ion concentrations on the in vitro reactions of bioactive glass 45S5 particles, Int. J. Appl. Glass Sci. 13 (2022) 695–707, https://doi.org/10.1111/ijag.16579.
[34] T. Kokubo, H. Takadama, How useful is SBF in predicting in vivo bone bioactivity? Biomaterials 27 (2006) 2907–2915, https://doi.org/10.1016/j.biomaterials.2006.01.017.
[35] M. Bohner, J. Lemaitre, Can bioactivity be tested in vitro with SBF solution? Biomaterials 30 (2009) 2175–2179, https://doi.org/10.1016/j.biomaterials.2009.01.008.
[36] ISO - ISO 23317, Implants for surgery — in vitro evaluation for apatite-forming ability of implant materials, n.d, https://www.iso.org/standard/65054.html, 2014. (Accessed 6 June 2022).
[37] H.S. Sidhu, M.I. Nelson, E. Balakrishnan, An analysis of a standard reactor cascade and a step-feed reactor cascade for biological processes described by monod kinetics, Chem. Prod. Process Model. 10 (2015) 27–37, https://doi.org/10.1515/cppm-2014-0022.
[38] New England Biolabs Inc, pH vs temperature for tris buffer, n.d, https://international.neb.com/tools-and-resources/usage-guidelines/ph-vs-temperature-for-tris-buffer, 2020. (Accessed 7 February 2022).
[39] I.D. Xynos, A.J. Edgar, L.D.K. Buttery, L.L. Hench, J.M. Polak, Ionic products of bioactive glass dissolution increase proliferation of human osteoblasts and induce insulin-like growth factor II mRNA expression and protein synthesis, Biochem. Biophys. Res. Commun. 276 (2000) 461–465, https://doi.org/10.1006/bbrc.2000.3503.
[40] J.-Y. Sun, Y.-S. Yang, J. Zhong, D.C. Greenspan, The effect of the ionic products of Bioglass® dissolution on human osteoblasts growth cycle in vitro, J Tissue Eng Regen Med 1 (2007) 281–286, https://doi.org/10.1002/term.34.
[41] A. Hoppe, N.S. Güldal, A.R. Boccaccini, A review of the biological response to ionic dissolution products from bioactive glasses and glass-ceramics, Biomaterials 32 (2011) 2757–2774, https://doi.org/10.1016/j.biomaterials.2011.01.004.
[42] S. Fagerlund, J. Massera, N. Moritz, L. Hupa, M. Hupa, Phase composition and in vitro bioactivity of porous implants made of bioactive glass S53P4, Acta Biomater. 8 (2012) 2331–2339, https://doi.org/10.1016/j.actbio.2012.03.011.
[43] A.C.M. Renno, P.S. Bossini, M.C. Crovace, A.C.M. Rodrigues, E.D. Zanotto, N. A. Parizotto, Characterization and in vivo biological performance of biosilicate, BioMed Res. Int. (2013) 1–7, https://doi.org/10.1155/2013/141427, 2013.
[44] S. Fagerlund, L. Hupa, M. Hupa, Comparison of reactions of bioactive glasses in different aqueous solutions, Adv. Bioceram. Biotechnol. 218 (2010) 101–113, https://doi.org/10.1002/9780470909898.ch11. USA: John Wiley & Sons, Ltd.
[45] M. Cerruti, D. Greenspan, K. Powers, Effect of pH and ionic strength on the reactivity of Bioglass® 45S5, Biomaterials 26 (2005) 1665–1674, https://doi.org/10.1016/j.biomaterials.2004.07.009.
[46] L. Björkvik, X. Wang, L. Hupa, Dissolution of bioactive glasses in acidic solutions with the focus on lactic acid, Int. J. Appl. Glass Sci. 7 (2016) 154–163, https://doi.org/10.1111/ijag.12198.
[47] R.K. Iler, The Solubility of Silica. Chem. Silica, John Wiley & Sons, 1979, pp. 30–49.